Fu and Holzbaur, http://www.jcb.org/cgi/content/full/jcb.201302078/DC1

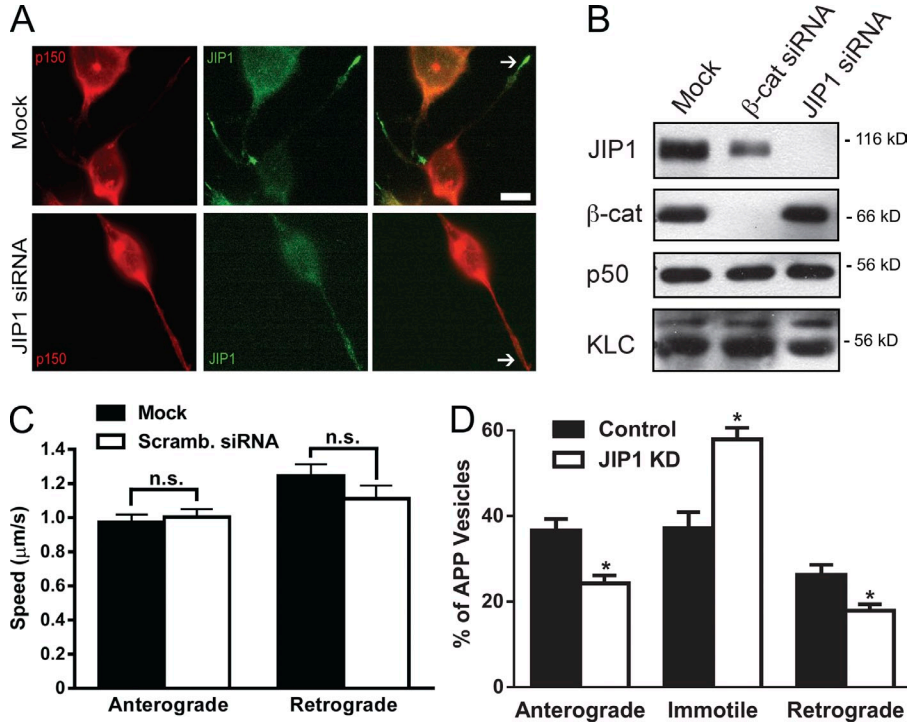

Figure S1. **JIP1 knockdown disrupts transport of APP-positive vesicles in neuronal CAD cells.** (A) Immunostaining of CAD cells with anti-JIP1 antibody shows efficient knockdown with JIP1 siRNA 48 h after transfection. Anti-p150 staining is shown as a reference for cell contour. Arrows point to distal neurites, where JIP1 accumulates under control conditions. Bar, 10 µm. (B) Western blot of CAD cells 48 h after transfection with JIP1 siRNA. β-Catenin siRNA is shown as a control. No compensatory changes are observed in expression of motor proteins p50 (a subunit of dynactin) and KLC upon JIP1 knockdown. (C) Sequence-specific scrambled siRNA showed no changes in anterograde ($P = 0.65$) or retrograde ($P = 0.20$) speed of APP-YFP transport in CAD cells (n = 19–27 cells). (C and D) Only JIP1 knockdown experiments assessed by immunofluorescence staining of parallel coverslips with >90% knockdown were imaged and analyzed. (D) JIP1 knockdown decreased the percentage of anterograde and retrograde APP-YFP vesicles in CAD cells (n = 27–31 cells). Error bars show the mean ± SEM; *, $P < 0.05$; n.s., not significant.

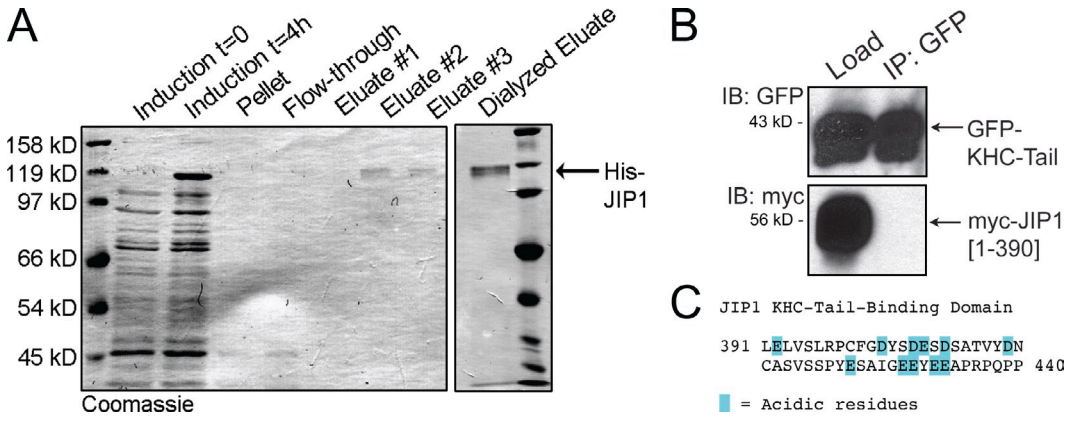

Figure S2. **The minimal KHC–tail-binding domain of JIP1 (aa 391–440) is highly acidic.** (A) Recombinant His-JIP1 was purified from *E. coli*. Coomassie-stained blot shows efficient induction of His-JIP1 in *E. coli* cultures with 1 mM IPTG for 4 h (first two lanes). Pellets were denatured in 8 M urea (third lane), purified using His-Bind Resin (EMD Millipore) and eluted with 500 mM imidazole (fourth through seventh lanes). Eluates were combined and concentrated by dialysis (Dialyzed eluate). (B) JIP1[1–390] does not bind to KHC tail. Lysates from COS7 cells cotransfected with myc-JIP1[1–390] and GFP-KHC-tail were immunoprecipitated with an anti-GFP antibody. No detectable myc-JIP1[1–390] coimmunoprecipitated with GFP-KHC-tail. (C) The minimal KHC–tail-binding domain of JIP1 (aa 391–440) contains 22% acidic residues.

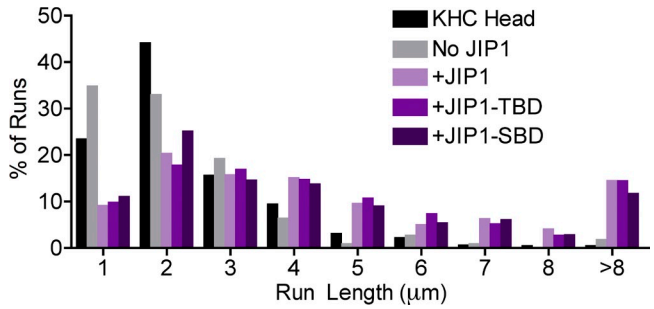

Figure S3. **JIP1 binding to KHC increases run length in vitro.** Histograms of run length distributions for constitutively active KHC-head-Halo or KHC-Halo in the presence of JIP1, JIP1-TBD, or JIP1-SBD in in vitro TIRF motility assays. Data shown are pooled from three or more independent experiments per condition (n = 52–181 microtubules and n = 109–758 runs).

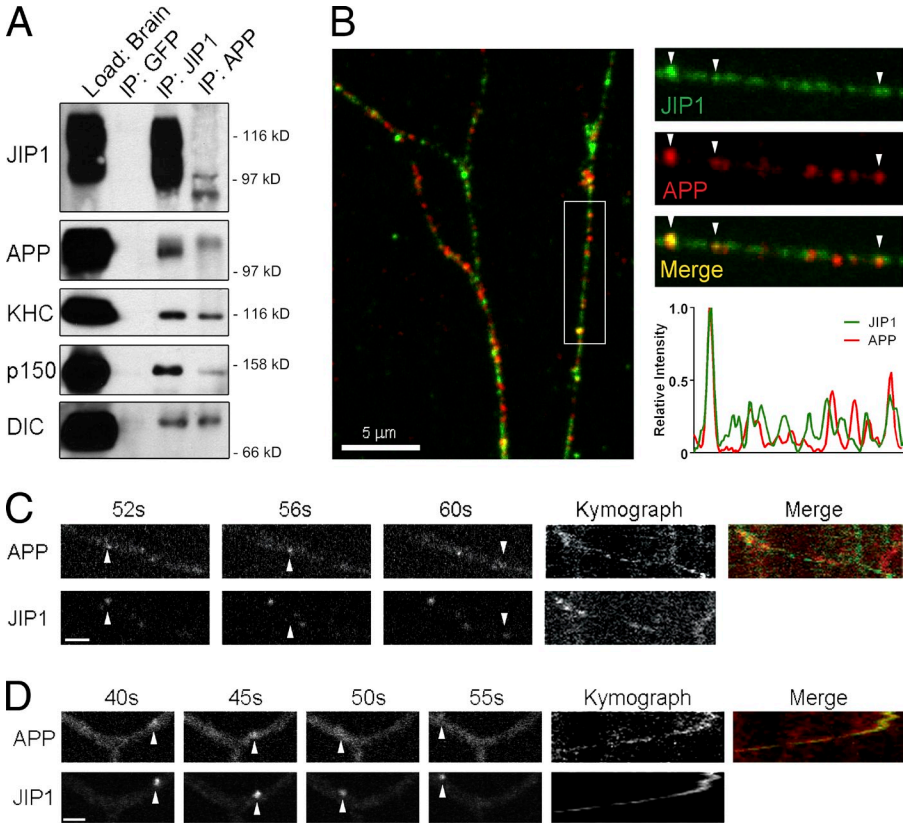

Figure S4. **Endogenous APP and JIP1 form functional transport complexes with anterograde and retrograde motors.** (A) Endogenous JIP1 and APP coimmunoprecipitate with KHC, p150^{Glued}, and dynein intermediate chain (DIC) in mouse brain homogenate. Interestingly, immunoprecipitation with a monoclonal APP antibody (2C11; EMD Millipore) selectively coimmunoprecipitated the lower molecular mass band of JIP1. (B) Endogenous JIP1 and APP colocalize on vesicles along axons in nontransfected DRGs. Representative image shows immunofluorescence staining of JIP1 (green) and APP (red). The boxed region is enlarged and analyzed by line scans to demonstrate individual vesicles on which JIP1 and APP are colocalized (arrowheads). (C) Fluorescently tagged JIP1 and APP comigrate on anterograde moving vesicles in DRGs. DRGs were transfected with APP-YFP and Halo-JIP1 and treated with red HaloTag TMR ligand at 37°C for 15 min and imaged at approximately one frame per second with a confocal microscope. Arrowheads depict comigrating APP-YFP and Halo-JIP1. Bar, 2 μm. (D) Fluorescently tagged JIP1 and APP comigrate on retrograde moving vesicles in DRGs. DRGs were transfected with APP-DsRed and EGFP-JIP1 and imaged at one frame per second with a confocal microscope. Arrowheads depict comigrating APP-DsRed and EGFP-JIP1. Bar, 2 μm.

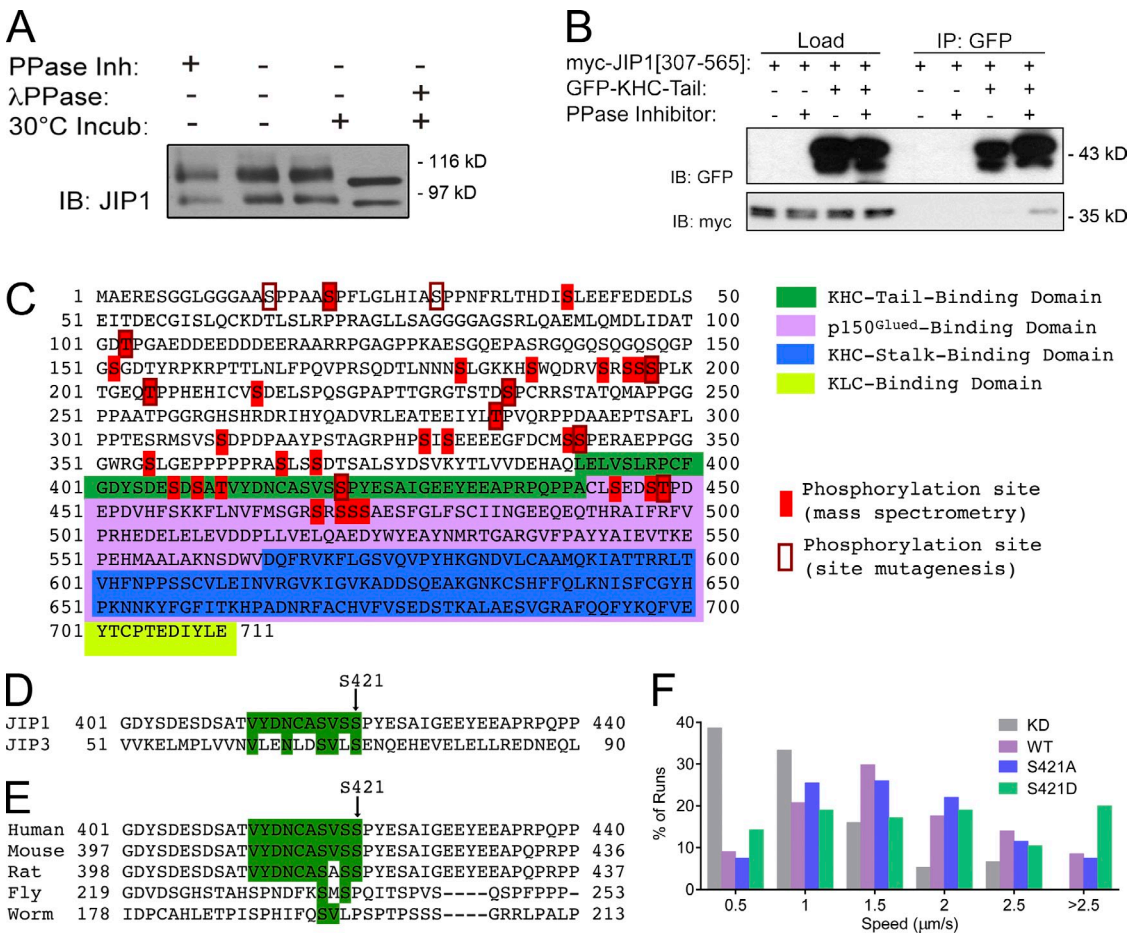

Figure S5. **JIP1 phosphorylation and KHC tail binding.** (A) JIP1 from mouse brain lysate is phosphorylated. Incubation of brain lysate at 30°C for 30 min with λ phosphatase (200 U/100 µg protein) dephosphorylates JIP1. Similar results were observed with alkaline phosphatase treatment (not depicted). (B) KHC tail preferentially binds to phosphorylated myc-JIP1[307–565]. Immunoprecipitation with an anti-GFP antibody of lysates of COS7 cells cotransfected with GFP-KHC-tail and myc-JIP1[307–565] selectively pulled down a phospho-JIP1[307–565] band in the presence of phosphatase inhibitors. (C) Summary of known phosphorylation sites in human JIP1. Phosphorylation sites identified by mass spectrometry (D'Ambrosio et al., 2006) are highlighted in red and those confirmed by site-directed mutagenesis to be directly phosphorylated by JNK in vitro (Nihalani et al., 2003) are boxed in dark red. (D) The region around JIP1-S421 is heavily conserved in mammals. (E) The region around JIP1-S421 may represent a 10-aa consensus motif for KHC binding, as it is 50% conserved in the minimal KHC-binding domain (aa 50–80) of the motor adaptor protein JIP3. (F) Histogram of APP speeds in neurons expressing JIP1 phosphomutants. Data represents three independent experiments (n = 7–9 neurons and n = 78–224 runs).

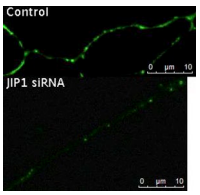

Video 1. **JIP1 depletion disrupts APP-YFP motility in DRGs.** Mouse DRGs were transfected with APP-YFP and JIP1 siRNA and observed at 2 DIV in Hibernate A medium at 37°C. In the control (top), anterograde motility is directed toward the left and retrograde motility is directed toward the right. In the JIP1 knockdown (bottom), anterograde motility is directed toward the right and retrograde motility is directed toward the left. Images were acquired at 250 ms per frame for 1 min using an epifluorescence microscope (DMI6000B; Leica); playback speed is 10× real time (40 frames per second).

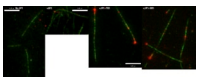

Video 2. **JIP1 activates KHC-Halo motility in a single molecule TIRF assay.** (left to right) KHC-Halo alone (no JIP1), KHC-Halo +myc-JIP1, KHC-Halo +myc-JIP1-TBD (aa 285–440), and KHC-Halo +myc-JIP1-SBD (aa 554–711). Flow chambers contain KHC-Halo-TMR (red) and microtubules (green). Images were acquired at room temperature at three frames per second for 1 min on a spinning disk TIRF microscope (Ultraview Vox system [PerkinElmer] with Ti body [Nikon]); playback speed is 10× real time (30 frames per second).

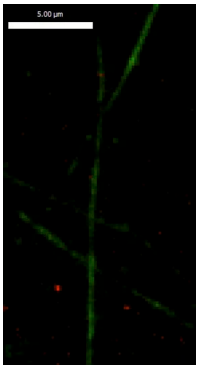

Video 3. **Addition of FLAG-p150^{Glued}-CBD inhibits JIP-mediated enhancement of KHC-Halo motility in a single molecule TIRF assay.** Flow chambers contain premixed myc-JIP1 and FLAG-p150^{Glued}-CBD COS7 lysates that were added to KHC-Halo-TMR lysates (red) and microtubules (green). Images were acquired at room temperature at three frames per second for 1 min on a spinning disk TIRF microscope (Ultraview Vox system [PerkinElmer] with Ti body [Nikon]); playback speed is 10× real time (30 frames per second).

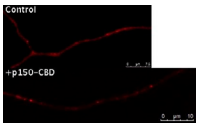

Video 4. **Expression of p150^{Glued}-CBD disrupts APP-DsRed transport in DRGs.** Mouse DRGs were transfected with APP-DsRed and a bicistronic vector coexpressing FLAG-p150^{Glued}-CBD and GFP and observed at 2 DIV in Hibernate A medium at 37°C. Anterograde motility is directed toward the left and retrograde motility is directed toward the right. Images were acquired at 250 ms per frame for 1 min using an epifluorescence microscope (DMI6000B; Leica); playback speed is 10× real time (40 frames per second).

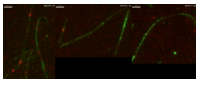

Video 5. **Phosphorylations mutants at JIP1-S421 alter KHC activation in vitro.** (left to right) KHC-Halo-TMR with wild-type myc-JIP1, myc-JIP1-S421A, and myc-JIP1-S421D. Flow chambers contain KHC-Halo-TMR (red) and microtubules (green). Images were acquired at room temperature at three frames per second for 1 min on a spinning disk TIRF microscope (Ultraview Vox system [PerkinElmer] with Ti body [Nikon]); playback speed is 10× real time (30 frames per second).

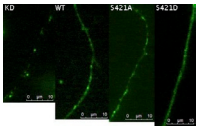

Video 6. **Phosphorylation mutants at JIP1-S421 selectively enhance APP transport in one direction in DRGs.** Mouse DRGs were transfected with APP-YFP and JIP1 siRNA and rescued with a bicistronic vector coexpressing human JIP1 (wild type, S421A, or S421D), and then observed at 2 DIV in Hibernate A medium at 37°C. (left to right) JIP1 knockdown and rescue with wild-type JIP1, JIP1-S421A, or JIP1-S421D. Anterograde motility is directed toward the top, whereas retrograde motility is directed toward the bottom. Images were acquired at 250 ms per frame for 1 min using an epifluorescence microscope (DMI6000B; Leica); playback speed is 10× real time (40 frames per second).

References

Nihalani, D., H.N. Wong, and L.B. Holzman. 2003. Recruitment of JNK to JIP1 and JNK-dependent JIP1 phosphorylation regulates JNK module dynamics and activation. *J. Biol. Chem.* 278:28694–28702. http://dx.doi.org/10.1074/jbc.M304212200

D'Ambrosio, C., S. Arena, G. Fulcoli, M.H. Scheinfeld, D. Zhou, L. D'Adamio, and A. Scaloni. 2006. Hyperphosphorylation of JNK-interacting protein 1, a protein associated with Alzheimer disease. *Mol. Cell. Proteomics*. 5:97–113.